Gen Relativ Gravit (2015) 47:129
DOI 10.1007/s10714-015-1975-4

RESEARCH ARTICLE

Initial condition dependence and wave function confinement in the Schrödinger–Newton equation

Marion Silvestrini[1] · **Leonardo G. Brunnet**[1] · **Marcelo Disconzi**[2] · **Carolina Brito**[1]

Received: 1 September 2015 / Accepted: 29 September 2015 / Published online: 10 October 2015

Abstract In this work we study the dynamics of the Schrödinger–Newton (SN) equation upon different choices of initial conditions. Setting up superpositions of Gaussian-like wave packages, a very rich behavior for the critical mass as a function of the parameters of the problem is observed. We find that, for certain values of the parameters, the critical mass is smaller than the critical mass for the system whose initial condition is a single Gaussian wave package, which was the situation previously investigated in the literature. This opens a possibility that more complex initial conditions could in fact produce a significant decrease in the value of the critical mass, which could imply that the SN approach could be tested experimentally. Our conclusions rely on both numerical and analytic estimates. Furthermore, a detailed numerical study is carried out in order to investigate finite-size effects on the simulations, refining earlier results already published. In order to facilitate the reproducibility of our results, a detailed description of our numerical methods has been included in the presentation.

Electronic supplementary material The online version of this article (doi:10.1007/s10714-015-1975-4) contains supplementary material, which is available to authorized users.

✉ Carolina Brito
carolina.brito@ufrgs.br

Marion Silvestrini
marion.silvestrini@ufrgs.br

Leonardo G. Brunnet
leon@if.ufrgs.br

Marcelo Disconzi
marcelo.disconzi@vanderbilt.edu

[1] Physics Department, Universidade Federal do Rio Grande do Sul, Av. Bento Gonalves 9500 - Caixa Postal 15051, Porto Alegre, RS CEP 91501-970, Brazil

[2] Department of Mathematics, Vanderbilt University, Nashville, TN, USA

Keywords Schrödinger–Newton Equation · Semi-classical gravity · Critical mass · Wave function confinement · Gravitational inhibition

Contents

1 Introduction and statement of the results

Consider the Schrödinger-Newton equation

$$i\hbar \frac{\partial \Psi(t,x)}{\partial t} = \left(-\frac{\hbar^2}{2m}\Delta - Gm^2 \int_{\mathbb{R}^3} \frac{|\Psi(t,y)|^2}{|x-y|}\, dy \right) \Psi(t,x), \tag{1}$$

where $\hbar$ is Planck's constant; G is Newton's constant; m is a real-valued parameter representing the mass; $i^2 = -1$; Δ is the Laplacian in $\mathbb{R}^3$; and Ψ is the wave-function, a complex-valued function in $\mathbb{R}^4$ of unit norm in $L^2(\mathbb{R}^3)$. Here, $\mathbb{R}^4$ is physically thought of as time and space, $\mathbb{R}^4 = \mathbb{R} \times \mathbb{R}^3$, with coordinates denoted by (t, x), where t is time and x the spatial position. For background on Eq. (1), see Sect. 1.1 below. Here, let us simply point out that Eq. (1) is based on some rather intriguing hypotheses about the coupling of gravity with matter, leading to a description of certain non-relativistic quantum-mechanical systems that differs from that provided by the ordinary Schrödinger equation. Thus, assessing the correctness of Eq. (1) can potentially provide a phenomenological window into the elusive subject of the behavior of gravity in the presence of quantum effects.

From a quick heuristic analysis of Eq. (1), it is seen that when $m \gg 1$, the dynamics will be dominated by gravity, i.e., by the term proportional to G, and by the diffusion, i.e., the term involving Δ, when $m \ll 1$. Thus, it is natural to expect that there exists a value of m, henceforth called the *critical mass* and denoted m_c, for which the gravitational and the diffusive terms are "balanced". Previous works refer to m_c as a mass value above which the package "collapses" [54], or a value below which the dispersion is "gravitationally inhibited" [26]. Experimentally observing such a collapse would be tantamount to verifying a prediction based on the Schrödinger-Newton equation, hence suggesting the validity of the underlying assumptions that lead to Eq. (1) (some of such assumptions are discussed in Sect. 1.1 below). It becomes, therefore, important to estimate m_c quantitatively, particularly if such an estimate yields values of mass accessible to current technology.

Naturally, an initial condition $\Psi(0, x)$ has to be provided in order to solve Eq. (1), and one expects that m_c will depend upon $\Psi(0, x)$. When the initial condition is a (radially symmetric) Gaussian of width σ, the value of m_c has been investigated initially by Carlip and Salzman [50], and subsequently in more detail by Giulini and Großardt [26] and Meter [54]. They found that m_c is of the order $\left(\frac{\hbar^2}{G\sigma}\right)^{\frac{1}{3}} \equiv m_r$. With this estimate at hand, we can in principle test Eq. (1) experimentally by evolving a quantum-mechanical system of mass $m \gtrsim m_c$ whose wave function at $t = 0$ is as just described. If, under these conditions, the wave-function of the system remains confined in a region of space rather than spreading out as predicted by standard quantum mechanics (or if the spreading is gnificantly slower than that predicted by the Schrödinger equation for a free particle), then we would have found evidence favoring a description based on the Schrödinger-Newton equation. Actually implementing this procedure, however, is technically challenging in that one has to construct, in a lab, a physical system that is described in terms of a wave-function of width σ, having a mass of the order m_c, and for which, at the same time, quantum-mechanical effects can be precisely measured. To understand where the difficulty lies, one simply has to point out that systems whose quantum mechanical nature is manifest in lab experiments tend to have very tiny masses and wave-packages of small width, a situation that precludes $m \gtrsim \left(\frac{\hbar^2}{G\sigma}\right)^{\frac{1}{3}}$. This is the case even when one considers the so-called "heavy" systems for which quantum effects can still be experimentally observed. For instance, current day molecular interferometry technology allows experimentalists to build systems corresponding to wave-packages of size $\sigma \sim 0.5\mu m$ and masses as large as $m \sim 10^3 u$ [3,31]. This is still, however, several orders of magnitude below the corresponding m_c for $\sigma \sim 0.5\mu m$, namely, $m_c \sim 10^9 u$.

In light of the above, an obvious question is whether it is possible to find initial conditions that produce smaller values for m_c. In other words, dependence of m_c on $\Psi(0, x)$ raises the possibility that there exist initial conditions that lead to values m_c closer to what can be achieved in actual experiments of quantum mechanical systems. This is the problem addressed in this manuscript.

We take as $\Psi(0, x)$ a superposition of a Gaussian peaked at the origin and a Gaussian-like function peaked away from the origin. By Gaussian-like, we mean a radially symmetric function that is in fact a Gaussian centered at some $R > 0$ with respect to the radial variable r, i.e., a function of the form $\sim e^{-\frac{(r-R)^2}{2\sigma^2}}$. Obviously, such a function is not a Gaussian in $\mathbb{R}^3$ (unless $R = 0$), but it retains the Gaussian features of being radially symmetric and peaked at R. While a superposition of two actual Gaussian would also sound natural, this would break radial symmetry when one of them is not centered at the origin, making the analytic and numerical estimates more difficult. Figure 1 illustrates our initial conditions. We notice that simply taking $e^{-\frac{(r-R)^2}{2\sigma^2}}$ rather than a superposition will not have the desired effect of lowering m_c (see Sect. 1).

Main result. Putting $\psi_R = e^{-\frac{(r-R)^2}{2\sigma^2}}$, we write explicitly $\Psi(0, x) = A(\psi_0 + \psi_R)$, where A is a normalization constant and $\psi_0 = e^{-\frac{r^2}{2\sigma^2}}$. We investigate how m_c varies

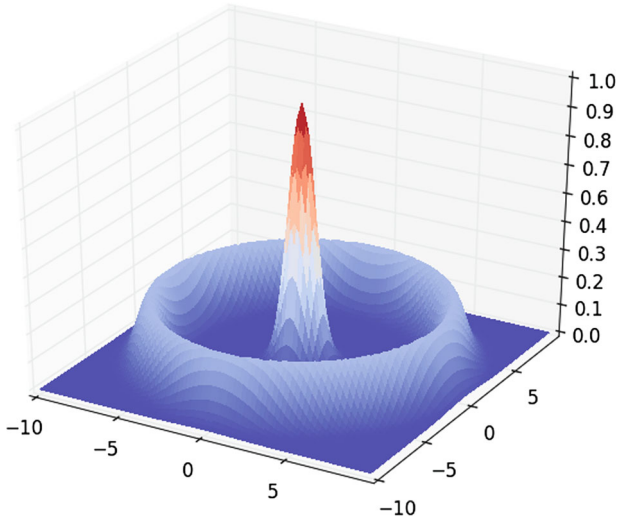

Fig. 1 Illustration of a typical initial condition

with the separation R between the two peaks. The results are summarized in Fig. 5, where m_c is plotted, in units of m_r, as a function of R. The two curves in Fig. 5 represent the analytic and numerical estimates. Both agree qualitatively, with the quantitative discrepancy probably stemming from some of the rough approximations we have employed in the analytic calculations as discussed below. Our results show that m_c decreases in comparison to m_r for certain choices of R. While this decrease is barely by an order of magnitude, thus still far from what is needed to reach values of masses achievable in lab experiments in the foreseeable future, the main message here is that *it is possible to obtain values of* m_c *less than* $m_r \equiv \left(\frac{\hbar^2}{G\sigma}\right)^{\frac{1}{3}}$ *upon suitable choices of initial conditions.* This raises the interesting *possibility that more complex initial conditions could in fact produce a significant decrease in the value of* m_c.

Figure 5 also shows that the critical mass of our system approaches m_r when $R \gg 1$. This behavior is discussed in detail in the "Appendix 4". In a nutshell, when R becomes very large, the system "decouples" into two subsystems associated with ψ_0 and ψ_R. For ψ_R, a very large value of m is necessary to prevent the system from spreading, thus, ψ_0 is solely responsible for the confining behavior when $m = m_c$. Therefore, noticing that, by construction, $m_c = m_r$ when $R = 0$, it can be concluded that the observed *lowering of the critical mass in relation to* m_r *is a consequence of the interaction of the parts of* $\Psi(t, x)$ *associated with* ψ_0 *and* ψ_R. In physical terms, this can be understood as follows. For $R \gg 1$, the gravitational interaction between the packages concentrated near zero and near R is negligible, and thus confinement can only happen due to the self-interaction of each of these packages. However, when the two packages are near each other, not only does their self-gravitational interaction work against the diffusive term, but their mutual interaction also contributes to the confinement. This raises the obvious question of what happens when several (i.e., more than two) packages are employed, but this is not addressed in this work.

Notice that the question of whether wave functions whose associated probability density resembles some given intricate initial condition (or even our $\Psi(0, x)$) can be realized in laboratories is left untouched here. If it turns that such constructions seem out of reach, this would definitely diminish the appeal for the investigations we have carried out. On the other hand, we should not underestimate the ability of experimentalists in producing actual far-reaching quantum states of matter, as many recent advances have demonstrated [3,8].

A second question addressed in this paper is that of the robustness of earlier numerical results. Although the estimate $m_c \sim \left(\frac{\hbar^2}{G\sigma}\right)^{\frac{1}{3}}$ for a single wave-packet as initial condition has been independently verified by Giulini and Großardt [26] and Meter [54], and their results agree with standard analytic estimates, leaving little doubt about the correctness of their results, we believe that a third and more thorough verification is beneficial. This seems appropriate especially in light of finite-size effects that inevitably plague numerical simulations. Such effects have not been reported in Giulini and Großardt, and have been dealt with by Meter via a clever, albeit artificial, choice of boundary conditions. In this regard, it is perhaps worthwhile to remember that the first reported numerical results concerning m_c were very crude [50], and it took about five years after [50] for a coherent and more reliable picture to emerge. Such caution is particularly important when one takes into account the non-linear and non-local nature of Eq. (1). Reassuringly, although by no means surprisingly, our results confirm those of [26,54].

We finish this section with an important conceptual consideration. We find that the regime where the gravitational interaction becomes relevant involves large values of mass, as indicated in Fig. 5. Such values of mass can only occur in large systems, such as the type of heavy molecules previously referred to, requiring a description of multi-particle systems. On the other hand, we are considering the dynamics of a single mass distribution self-interacting via Eq. (1). In order to make these two ideas compatible, one has to work with systems where the multi-particle dynamics can be reduced to that of its center-of-mass, with the latter described by Eq. (1). The dynamics of the center-of-mass has been analyzed by Giulini and Großardt in [28]. They found that if the extent of an object is small in comparison to the uncertainty in localisation of its centre of mass, then Eq. (1) provides a good approximation for the dynamics of the multi-particle system, and our results should be understood in this context. See also the discussion in [1].

1.1 Background

In this section we describe some of the reasoning leading to Eq. (1), and specialists may want to skip this section.

As it is well-known, reconciling Einstein's General Theory of Relativity and Quantum Mechanics is one of the main open problems in contemporary Theoretical Physics. Whether this has to be achieved by finding a suitable theory of quantum gravity or by modifying Quantum Mechanics in a way that would allow it to be consistently coupled to classical General Relativity (or some other, more general, theory of gravity), is still an open question, although many plausible arguments point in the direction of the

former alternative, which also seems to be the consensus among the majority of the physics community. See, e.g., [10,52,55,56] for a general discussion.

If one assumes that gravity is quantized, then the outstanding success of General Relativity implies that quantum aspects pertaining to the gravitational field are negligible in most phenomena presently accessible to observation. However, it is expected that quantum gravity becomes important in the presence of extremely strong gravitational fields, such as those believed to exist in the interior of black hole event horizons and in the early universe. Unfortunately, despite much progress over the decades,[1] we still lack a robust theory of quantum gravity that could be used to make indirect, yet sufficiently accurate, predictions to match with observations. And due to the energy scales involved, direct measurements of quantum gravitational phenomena seem to be out of the question for generations to come, if not forever.

Given such a state of affairs, it seems natural to use some sort of semi-classical approximation to try to understand general features of how gravity interacts with matter. One hopes to be able to construct semi-classical models that retain enough features of the underlying full-fledged quantum description as a way of extracting information that can help us to constrain current theories of quantum gravity. For instance, despite being derived in a semi-classical formalism, the Hawking radiation [32] is an important guide to quantum theories of gravity, so that the ability to reproduce it becomes one of the first tests to any theory that attempts to quantize the gravitational field.

In such semi-classical approaches, one describes the gravitational field classically, but imposes quantum behavior on the matter present in the model in question. Specifying how matter interacts gravitationally is one of the main aspects of the model, and different choices are available. The most common choices rely on Quantum Field Theory on Curved Backgrounds, where one performs field quantization in a spacetime background that satisfies Einstein's equations. The matter-gravity interaction is described via a minimal coupling, with backreaction effects on the metric tensor generally (but not always) ignored. See the monographs [7,23,39,55] for an in-depth exposition, or the introduction in [17] for a short discussion. While this approach is very natural, it is technically challenging, thus one may ask if there are further simplifications that can lead to more tractable models.

One further simplification would be to consider non-relativistic models. As the non-relativistic limits of Quantum Field Theory and General Relativity are, respectively, ordinary Quantum Mechanics and Newtonian gravity, one possibility is to consider quantum matter that interacts gravitationally via a Newtonian gravitational potential. This is the situation described by the Schrödinger–Newton equation. Its physical content is as follows. Consider a spatially extended mass distribution that self-interacts gravitationally according to Newton's law of gravity. Denoting the total mass by m

[1] Any list of references on this is doomed to be very incomplete, but we mention the following works. For standard treatments of String Theory and its relation to the quantization of the gravitational field, see [30,45], or [5] for a more recent monograph. Attempts at constructing semi-realistic models out of String Theory and the related problems of stabilization and de Sitter vacua can be found in [2,9,16,19–22,29,33,53] and references therein, while connections with cosmology are explored in [4] and their references. For approaches based on Loop Quantum Gravity, see [48,49], or the recent survey [13], and references therein. For approaches based on Twistors, see [40,41,44] and references therein.

and the mass density function by ρ_m, the gravitational potential Φ satisfies

$$\Delta\Phi = 4\pi G\rho_m,$$

where G is Newton's constant. Suppose that the matter in the above equation is described quantum mechanically, in the sense that the time-evolution determines only the probability of finding an amount δm of the mass within a volume δV in space, and that such probability is given by the ordinary Schrödinger equation. In this case, the probability density, ϱ, is given by

$$\varrho = |\Psi|^2,$$

where the probability density and the mass density are linked through mass by $\varrho\, m = \rho_m$ and Ψ is a wave-function satisfying Schrödinger's equation with a potential given by Φ,

$$i\hbar\frac{\partial\Psi}{\partial t} = \left(-\frac{\hbar^2}{2m}\Delta + m\Phi\right)\Psi.$$

Combining the above, we obtain the Schrödinger–Newton equation Eq. (1).

Several remarks are in place. In considering the above reasoning, a specific assumption about the behavior of gravity coupled to matter in the quantum-mechanical realm is made. It consists of a modification of Schrödinger's equation, allowing for self-interaction inasmuch a massive particle is present, regardless of the existence of an external potential. In particular, the concept of free particles no longer exists. Such a modification, it should be noticed, is not excluded by current theoretical and experimental understandings of quantum mechanics because (a) we do not know precisely what quantum gravity is, and, therefore, the details of its possible semi-classical regimes are open to exploration; and (b) consequently, the limits where a semi-classical description is valid are not known either. Furthermore, it should come as no surprise that the Schrödinger equation is replaced by a more accurate description of quantum mechanical behavior once a more fundamental theory of gravity coupled to matter is formulated. The real question is whether this modification looks like Eq. (1) in some appropriate limit. Regarding this question, what makes the Schrödinger–Newton equation interesting is that the scales involved are far more modest than those of full-fledged theories of quantum gravity, even in the face of the aforementioned gap between known values of m_c and current technology. This is one of the reasons why Eq. (1) has recently attracted considerable attention (see, e.g., [11,26,28,50,54] and references therein). Recently, electromagnetic interactions have been added to the Schrodinger–Newton equation to include relativistic effects [37].

Although above we have given a motivation to study Eq. (1) on the basis of a semi-classical analysis, it ought to be stressed that the Schrödinger–Newton equation also plays an important role in some approaches that assume that gravity remains fundamentally classical at all levels, and in Penrose's discussion of the "collapse" of the wave-function [42,43] (although it should be stressed that the meaning of the term "collapse" here has nothing to do with the infamous "collapse of the wave-function").

We refer the reader to [28,54] for a more detailed discussion of the theoretical underpinnings of Eq. (1). In passing, we point out that Eq. (1) does follow from certain non-relativistic limits of the Einstein-Klein-Gordon or Einstein-Dirac systems [27].

We finish this section pointing out that the study of equation Eq. (1) has also spurred a great deal of activity in the mathematical community. See, e.g., [6,12,14,15,18,24,25,34–36,38,47,51].

2 Analytic estimate of the critical mass

In this section, we provide analytic estimates for the critical mass. We proceed essentially as in section 3.1 of [26], making the necessary adaptations for our initial condition. Unfortunately, some of the computations are extremely long, involving several page-long expressions (although they are by no means difficult, consisting essentially of derivatives and algebraic manipulations). Hence, we will describe the procedure, omitting some of the explicit expressions. The final expression for m_c is given in the "Appendix".

Consider the following wave function for a free particle of mass m (i.e., a solution to the ordinary Schrödinger equation):

$$\Psi_R(t,x)=\left(\sqrt{\pi}\left(1+\frac{i\hbar t}{m\sigma^2}\right)^{\frac{3}{2}}\sqrt{\sigma(2R\sigma e^{-\frac{R^2}{\sigma^2}}+\sqrt{\pi}(2R^2+\sigma^2)(1+\mathrm{Erf}(R/\sigma)))}\right)^{-1} \times e^{-\frac{(r-R)^2}{2\sigma^2\left(1+\frac{i\hbar t}{m\sigma^2}\right)}}, \tag{2}$$

where Erf is the error function and $r^2=|x|^2$. Thus, $\Psi_R(0,x)$ has the form described in the introduction, $e^{-\frac{(r-R)^2}{2\sigma^2}}$ up to a normalization factor. Naturally, Ψ_R reduces to the usual free-particle solution with a Gaussian initial condition when $R=0$. In fact, the calculations below reduce to those in section 3.1 of [26] when $R=0$.

Define

$$\Psi(t,x)=A\,(\Psi_0(t,x)+\Psi_R(t,x)),$$

where A is a normalization constant. By the linearity of the Schroödinger equation, Ψ is a solution with initial condition $\Psi(0,x)\sim e^{-\frac{r^2}{2\sigma^2}}+e^{-\frac{(r-R)^2}{2\sigma^2}}$. The radial probability density associated with $\Psi(t,x)$ is

$$\varrho_{\mathrm{rad}}(t,r)=4\pi r^2|\Psi(t,x)|^2.$$

In principle, differentiating ϱ_{rad} with respect to r, we can find the critical points of ϱ_{rad}, and in particular the value of r for which ϱ_{rad} has a global maximum, henceforth called r_p (it can be inspected graphically that such a maximum in fact exists). It is a function of t, i.e., $r_p=r_p(t)$. It also depends, of course, on the other parameters of the problem, σ, R, m, and $\hbar$, but this dependence will be omitted in order to simplify the notation.

Unfortunately, the expressions involved in this procedure are too complicated and it is unlikely that r_p can be found explicitly as a function of t, as in the case where $R = 0$. Since the acceleration of the density's peak, $\ddot{r}_p$, is needed to estimate m_c, we will proceed as follows (recall that we are following the ideas of [26]).

Because r_p is a critical point of ϱ_{rad}, it satisfies

$$\frac{\partial \varrho_{\text{rad}}(t, r_p)}{\partial r} = 0, \tag{3}$$

where the above means $\frac{\partial \varrho_{\text{rad}}(t,r)}{\partial r}$ evaluated at r_p, i.e., $\frac{\partial \varrho_{\text{rad}}(t,r)}{\partial r}\Big|_{r=r_p}$. Differentiating Eq. (3) twice in time, and solving for $\ddot{r}_p$, we obtain $\ddot{r}_p$ as a function of t, $\dot{r}_p$ and r_p, which we write symbolically as

$$\ddot{r}_p(t) = f(t, \dot{r}_p(t), r_p(t)).$$

Evaluating this expression at zero and using that $\dot{r}_p(0) = 0$, we obtain $\ddot{r}_p(0)$ as a function of $r_p(0)$, which again we write symbolically as

$$\ddot{r}_p(0) = f(r_p(0)).$$

Next, we need $r_p(0)$. Here, as before, we need to solve Eq. (3) for r, except that now we also set $t = 0$, and, again, we find that the resulting expression is too complicated to allow for an explicit solution. However, for the case $t = 0$, Eq. (3) simplifies considerably, so that $r_p(0)$ can be found numerically. We remark that Eq. (3), at $t = 0$, has more than one solution, but once the solutions are found it is easy to directly verify which one is the global maximum. Notice that $r_p(0)$, and therefore $\ddot{r}_p(0)$, is a function of σ, R, m, and $\hbar$, although this fact is obscured by the numerical procedure necessary to determine $r_p(0)$.

To find m_c, we set $\ddot{r}_p(0)$ equal to the Newtonian gravitational attraction given by $Gm/(r_p(0))^2$,

$$\ddot{r}_p(0) = \frac{Gm}{(r_p(0))^2}. \tag{4}$$

As $\ddot{r}_p(0)$ and $r_p(0)$ are functions of σ, R, m, and $\hbar$, we can solve for m in terms of the remaining parameters. Doing this for different values of R yields the first graph in Fig. 5.

We remark that this procedure gives an explicit expression for m_c in terms of σ, R, m, $\hbar$, and $r_p(0)$, which is given in the "Appendix 3". Indeed, from the above procedure, we obtain explicitly $\ddot{r}_p(0)$ in terms of $r_p(0)$, and thus Eq. (4) produces m_c as just stated after solving for m. It is only to find $r_p(0)$ that a numerical solution is needed. In particular, because such explicit expressions are available and a numerical algorithm had to be implemented solely to determine $r_p(0)$, we still characterize this argument as an "analytic" estimate of m_c. In fact, the procedure yielding $r_p(0)$ consists of a simple root finding for an algebraic equation. We thus reserve the the term "numerical" for methods that fully deserve this name, as the numerical solutions to Eq. (1) investigated in the next section.

Finally, it should be pointed out that the procedure described in this section involves the crucial approximation of eventually evaluating all the time-dependent quantities at time zero. While this is sensible, since one would expect that if gravity is going to confine $\Psi(t, x)$, this should happen at earlier times before the wave-function has spread out considerably, it is an approximation nonetheless. For the case $R = 0$, more accurate analytic tools are available in [26], but it seems that it would be far too complicated to implement them in our case. We believe that this approximation combined with the convoluted form of our initial conditions is responsible for the discrepancy between the analytic and numerical methods observed in Fig. 5.

3 Numerical methods

To study the time behavior of the Schrdinger-Newton equation, we solve equation Eq. (1) numerically using the initial conditions described above and illustrated in Fig. 1. We follow the numerical method used in [26], with the difference that units of mass, time and space are expressed in terms of $G, \hbar$ and σ, as in the reference [54]. The initial value of the width of the wave-package σ is the distance unit, $t_r = (\sigma^5/G\hbar)^{1/3}$ is the unit of time, and $m_r = (\hbar^2/G\sigma)^{1/3}$ is the unit of mass. The convenience of these units is that they exhibit the scale-invariance of the Schrodinger–Newton equation and reduce the problem to a single parameter, namely, the mass. If one replaces the mass by $m = m_r\,\tilde{m}$, $t = t_r\,\tilde{t}$ and $r = \sigma\,\tilde{r}$, the Eq. (1) can be written as

$$i\frac{\partial\Psi(\tilde{t},\tilde{r})}{\partial\tilde{t}} = \left(-\frac{1}{2\tilde{m}}\Delta + \tilde{m}\Phi(\tilde{t},\tilde{r})\right)\Psi(\tilde{t},\tilde{r}), \tag{5}$$

with

$$\Delta\Phi = 4\pi\tilde{m}|\Psi(\tilde{t},\tilde{r})|^2. \tag{6}$$

Hereafter, all results will be given in terms of the reduced units. The details necessary to reproduce our numerical results are explained in "Appendix 1". Here, we will discuss only two important aspects of the numerical solutions: the boundary and initial conditions

3.1 Boundary conditions

The system under study lives in an infinite space. However, the simulation box has to be finite and the outer boundary should be far enough from the origin in order to avoid reflection of the wave packet at the boundary. To solve this problem, Meter [54] uses Neumann boundary conditions in his simulations. This means that the part of the packet that touches the outer boundary is eliminated from the simulation domain. Here, we keep the system size big enough to avoid such reflections. In practice, a big system of size L is chosen and the simulation is run during an interval of time such that the wave packet calculated at the boundary is negligible. Explicitly:

$$\varrho_{\text{rad}}(\tilde{r} = L) \leq 10^{-8}.$$

3.2 Initial conditions

We use two different shapes for the wave packet as initial conditions. The first one initializes the system with a spherically symmetric Gaussian packet:

$$\Psi_0(\tilde{t}=0,\tilde{r}) = (\pi)^{-3/4}\, exp\left(-\frac{\tilde{r}^2}{2}\right). \tag{7}$$

This condition was introduced in previous works, [26,50,54], and here it is used to compare our simulations with previous numerical results. In references [26,54], a difference of about 20 % in the critical mass was found. We will comment on this in "Appendix 2".

The second initial condition is a combination of two Gaussians in the radial variable, as illustrated in Fig. 1:

$$\begin{aligned} \Psi(\tilde{t}=0,\tilde{r}) = &\quad \Psi_0(\tilde{r}) + \Psi_R(\tilde{r})\,, \quad \text{with} \\ \Psi_0(\tilde{r}) = &\quad A_1\, exp\left(-\frac{\tilde{r}^2}{2}\right)\,, \quad \text{and} \\ \Psi_R(\tilde{r}) = &\quad A_2\, exp\left(-\frac{(\tilde{r}-R)^2}{2}\right)\,, \end{aligned} \tag{8}$$

where A_0 is such that $\int_0^\infty \tilde{r}^2|\Psi_0|^2 d\tilde{r} = A$, A_2 is such that $\int_0^\infty \tilde{r}^2|\Psi_R|^2 d\tilde{r} = A$ and A such that $\int_0^\infty \tilde{r}^2|\Psi|^2 d\tilde{r} = 1$. Note that when $R = 0$ it reduces to the case with only one Gaussian, Eq. (7).

In the next section we describe the evolution of the system using this initial condition and compare the critical mass measured numerically with the result obtained analytically in Sect. 2.

4 Results

In this section we present the study of the evolution of the Schrödinger–Newton equation (5) using as initial condition the distribution expressed by Eq. (8). The distance, R, between the Gaussian peaks is left as a free parameter to explore the corresponding values for the critical mass, m_c. Also in this section, we describe the criterion to define the critical mass and compare the numerical results with the analytical predictions discussed in Sect. 2.

Figure 2 describes the system behavior as a function of time for the particular initial condition with a single Gaussian centered at the origin, Eq. (7). Two kinds of measures are shown in this figure: (a) the value of the peak r_p of the radial probability density, $\varrho_{\rm rad}(\tilde{r})$, as a function of time, and (b, c) plot of $\varrho_{\rm rad}(\tilde{r})$ as function of the position $\tilde{r}$ at different times for different values of m. These figures show clearly that there are two distinct regimes: one at small m where the packet diffuses and the other, at larger m when it oscillates. We can then define m_c as being the value of mass for which the system changes its behavior from diffusive to oscillatory. Nevertheless, from a

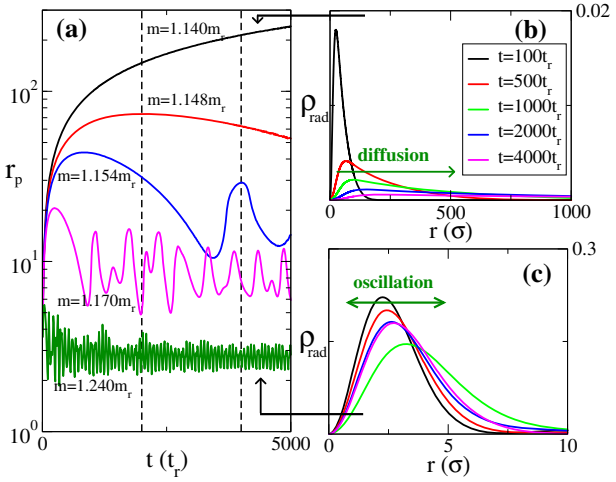

Fig. 2 Results for the case of a single gaussian $R = 0$. **a** The peak of the radial probability density $\varrho_{\rm rad}(\tilde{r}) = 4\pi\tilde{r}^2|\Psi|^2$, r_p, plotted against time for several masses, whose values are shown in the figure. *Vertical dashed lines* indicate the interval of time ΔT used to measure the average of r_p and define $\langle r_p \rangle$. **b** Radial probability density $\varrho_{\rm rad}$ as a function of $\tilde{r}$ at different times (specified in the legend) for $m = 1.14m_r$. **c** Radial probability density $\varrho_{\rm rad}$ as a function of $\tilde{r}$ at different times for $m = 1.24m_r$. *Each color* represents a different instant of time, which is specified in the legend of the figure. Distances are in units of σ and time in units of t_r. The system size is $L = 10^4\sigma$, $\Delta r = 0.01\sigma$ and $\Delta t = 0.01t_r$ (numeric parameters Δr and Δt are defined in "Appendix 1") (color figure online)

numerical point of view this definition is hard to fulfill. We then need a practical criterion that is defined in the following.

The quantitative definition of the critical mass m_c. The critical mass m_c is defined as the smallest value of mass for which the solution is oscillatory. We stress that this definition has some arbitrariness, because it depends on the interval of time ΔT during which one defines the average value of r_p, $\langle r_p \rangle$. Also, it has to be assured that the system size is big enough to avoid interference with the wave reflecting at the outer border of the system. Quantitatively, we chose the simulation time such that $\varrho_{\rm rad}(\tilde{r} = L) < 10^{-8}$. For the system size used in the case of Figs. 2 and 3, $L = 10^4\sigma$, one can safely use $\Delta T \in [2000t_r - 4000t_r]$. This interval is represented in the figures by the vertical lines.

Similar results as the ones shown in Fig. 2 were already reported in the references [26,54]. As already pointed out, these results differ by about 20 %, a point to which we return in "Appendix 2". The novelty here is that we go further and search m_c for other initial conditions. An example is given in Fig. 3, where we do the same analysis as in Fig. 2 but with an initial condition where there is one Gaussian at the origin and a second one at a distance $R = 5\sigma$. Qualitatively we observe the same behavior in both cases. The difference is quantitative: the critical mass m_c changes depending on the value of R.

We further simulate various initial conditions (in other words, different values of R) and, for each R, scan several values of mass. We then measure the average value of r_p during the interval ΔT and plot it as a function of m for different values of R. This

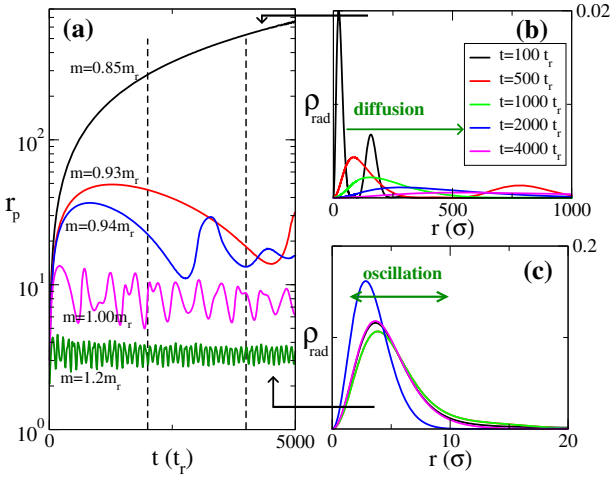

Fig. 3 Same measures as shown in Fig. 2, but here the results are for the initial condition with $R = 5\sigma$. **a** The peak of the radial probability density $\varrho_{\rm rad} = 4\pi\tilde{r}^2|\Psi|^2$, r_p, plotted against time for several masses. *Vertical dashed lines* indicate the interval of time ΔT used to measure the average of r_p. **b** Radial probability density $\varrho_{\rm rad}$ as a function of r at different times (specified in the legend) for $m = 0.85m_r$. **c** Radial probability density $\varrho_{\rm rad}$ as a function of $\tilde{r}$ at different times for $m = 1.20m_r$. *Each color* represents a different instant of time, which is specified in **b**. Distances are in units of σ and time in units of t_r. The system size is $L = 10^4\sigma$, $\Delta r = 0.01\sigma$, and $\Delta t = 0.01t_r$. The time evolution of the radial probability density for the masses exemplified in **b** and **c** are also shown in an animation in the supplementary material for time above $t = 100t_r$ (color figure online)

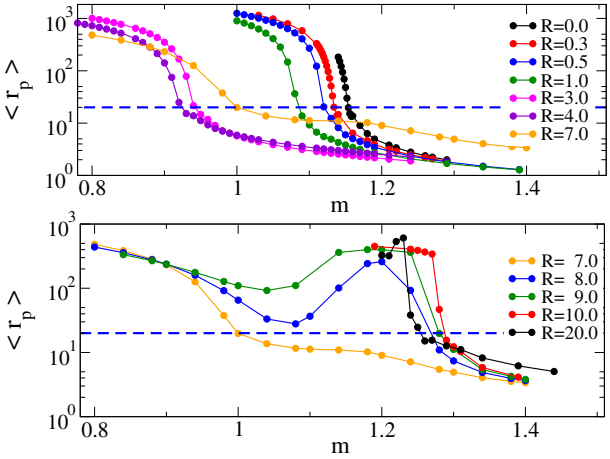

Fig. 4 Average value of r_p versus m for various initial conditions [different values of R, Eq. (8)]. The *dashed blue line* is the threshold limit to define m_c. $\langle r_p\rangle$ and R are measured in units of σ and m in units of m_r. $\langle r_p\rangle$ is defined during the interval $\Delta T \in [2000t_r, 4000t_r]$, which is indicated in Figs. 2 and 3 by the *vertical dashed lines* (color figure online)

is shown in Fig. 4. Note that in Fig. 4 we plot not only the cases where the solution is oscillatory but also when it is diffusive. It is clear that when the solution is diffusive, $\langle r_p\rangle$ is not representative of the behavior of the packet, since it keeps increasing during the measurement interval. For all R simulated, Fig. 4 shows a smooth behavior of $\langle r_p\rangle$

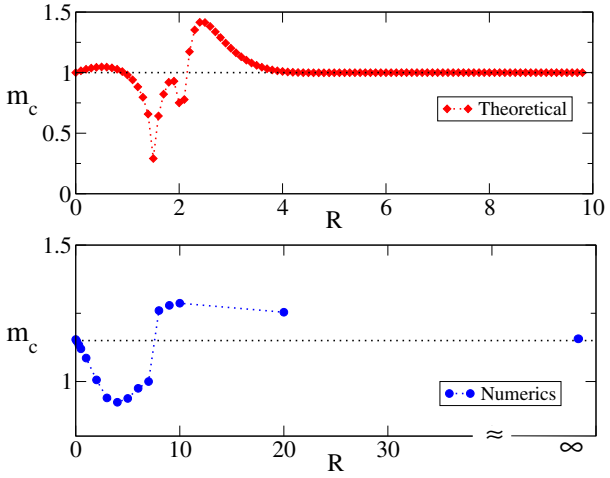

Fig. 5 The critical mass m_c as a function of the position R of the peak second Gaussian [Eq. (8)] for the theoretical computation in **a** and from numerical simulations in **b**. Note that the scale of distances are not the same in both figures because the agreement between the simulations and the analytical estimate is only qualitative, as discussed in the text. Masses are in units of m_r and R in units of σ

with m. In other words, there is no clear modification in the behavior of $\langle r_p \rangle$ for a given m that could suggest a clear definition of m_c. This pushes us to adopt the following criterion to quantitatively define m_c: For all R simulated we analyze the curves of r_p as a function of time, as exemplified in Figs. 2a and 3a, and we observed that, regardless the initial condition, when r_p passes a distance of $\approx 20\sigma$ from the origin, the packet does not come back again. We then define m_c as a value of mass at which $\langle r_p \rangle = 20\sigma$. We emphasize that this criterion involves a degree of arbitrariness, and it can depend on the system size or on the parameters $(\Delta t, \Delta r)$ of the simulation. However, the parameters $(L, \Delta t, \Delta r)$ have been varied and the essence of the wave packet behavior remained robustly the same.

Figure 5 summarizes the main result of this work. It shows how the value of the critical mass m_c varies when R changes from 0 to ∞ in an analytic estimate (Fig. 5a) and in the numerical simulations (Fig. 5b). Since the analytical estimate uses the initial shape of the wave packet, ignoring its dynamical evolution, it is not surprising that it has no *quantitative* agreement with the numerical simulations. However, the results from the theory and from the numerical simulations do share three interesting aspects: (i) the behavior of m_c is non-monotonic with R; (ii) in particular, m_c has a minimum value, denoted as m_c^{min}, that is smaller than m_c at $R = 0$; and (iii) when both Gaussians are very far from each other (limit of large R), the m_c is the same as in the case with only one Gaussian ($R = 0$). The point (iii) can be understood as a "decoupling" of the system into two weakly interacting subsystems when R is large. This is intuitively reasonable from the fact that the gravitational interaction decays with the distance, and it can be shown directly from Eq. (1). It is discussed in detail in "Appendix 4".

We stress that the main conclusions are robust against the exact criterion used to define m_c. We defined m_c as a value of mass at which $\langle r_p \rangle = 20\sigma$. From Fig. 4, we

observe that we could have chosen a slightly different threshold to define m_c, as, for example, $\langle r_p \rangle = 10\sigma$ or $\langle r_p \rangle = 30\sigma$. This would for sure change the absolute value of m_c, but it would not change the conclusions (i), (ii), and (iii) commented above.

Appendix 1: Details of the numerical methods

In this section we explain all the details necessary to solve the Eq. (5) numerically. We stress that the procedure used here is very similar to the one developed in the reference [26], but with the reduced variables used in [54]. We keep the same notation as in [26] as much as we can. We also note that, equation Eq. (5) is written in terms of the reduced variables $\tilde{m}$, $\tilde{t}$ and $\tilde{r}$. However, to simplify the notation, in this section we replace $\tilde{m} \to m, \tilde{t} \to t$; and $\tilde{r} \to r$.

For concreteness, we rewrite Eq. (5) in a suitable way:

$$i\frac{\partial \Psi}{\partial t} = H\Psi, \tag{9}$$

$$H = \frac{1}{2m}\Delta_r + m\Phi. \tag{10}$$

The formal solution of this equation is given by $\Psi(t, r) = e^{-iHt}\Psi(0, r)$. We observe that this is the solution when H does not depends on time t. In the case of Eq. (1), H depends on Ψ which depends on t. However, for the numerical solution we assume that the time discretization is small enough to consider Ψ as constant during it. The first step to solve Eq. (9) numerically is to discretize it in time and in space: time is written as $t = n\Delta t$ and the space as $r = j\Delta r$, where both j and n are integers, Δt is the time discretization, and Δr is the space discretization. The wave function is then denoted as $\Psi_j^n = \Psi(r = j\Delta r, t = n\Delta t)$. A numerical method to solve this equation needs to be both stable and unitary (required because the probability of finding a particle in the whole space should be constant). It is known that the Cayley's form for the finite-difference representation of e^{-iHt}, given by $\simeq \dfrac{1 - iH\Delta t/2}{1 + iH\Delta t/2}$, meets these two criteria [46]. This form leads to the following representation of the solution of the above equation:

$$\left(1 + \frac{1}{2}iH\Delta t\right)\Psi_j^{n+1} = \left(1 - \frac{1}{2}iH\Delta t\right)\Psi_j^n \,. \tag{11}$$

With algebraic manipulation, Eq. (11) can be expressed as

$$\Psi^{n+1} = \left[2\left(I + i\frac{\Delta t}{2}H\right)^{-1} - I\right]\Psi^n. \tag{12}$$

We then define the matrix Q,

$$Q = \frac{1}{2}\left(I + i\frac{\Delta t}{2}H\right), \tag{13}$$

and Eq. (12) can be simplified to

$$\Psi^{n+1} = \left(Q^{-1} - I \right) \Psi^n = \chi^n - \Psi^n, \tag{14}$$

where

$$\chi^n = Q^{-1} \Psi^n. \tag{15}$$

Setting up the matrix Q

To build the matrix Q, we need to handle the two terms of the hamiltonian represented by the Eq. (10): the Laplacian operator and the nonlinear term Φ.

The radial component of the Laplacian, Δ_r, in spherical coordinates is given by

$$\Delta_r = \begin{cases} \dfrac{\partial^2}{\partial r^2} + \dfrac{2}{r}\dfrac{\partial}{\partial r} & \text{if} \quad r > 0 \\ 3\dfrac{\partial^2}{\partial r^2} & \text{if} \quad r = 0, \end{cases} \tag{16}$$

which can be discretized in the following way,

$$\Delta \Lambda_j^n = \begin{cases} \dfrac{1}{(\Delta r)^2}\left(\dfrac{j-1}{j}\Lambda_{j-1}^n - 2\Lambda_j^n + \dfrac{j+1}{j}\Lambda_{j+1}^n \right) & \text{if} \quad j > 0 \\ \dfrac{1}{(\Delta r)^2}(-6\Lambda_0^n + 6\Lambda_1^n) & \text{if} \quad j = 0. \end{cases} \tag{17}$$

The second term of the Hamiltonian, Φ, is the solution of the Possion equation, Eq. (6). We apply the Green method to solve it [54]:

$$\phi = -\int_0^\infty G(\mathbf{r}, \mathbf{r}') |\Psi(r', t)|^2 dV',$$

where $G(\mathbf{r}, \mathbf{r}')$ is the Green function,

$$G(\mathbf{r}, \mathbf{r}') = \frac{1}{4\pi \, \max(r, r')}. \tag{18}$$

The result is given by

$$\phi = -4\pi m \left[\frac{1}{r} \int_0^r |\Psi(r', t)|^2 r'^2 dr' + \int_r^\infty |\Psi(r', t)|^2 r' dr' \right]. \tag{19}$$

The expression above can be discretized as

$$\phi_j^n = -4\pi m (\Delta r)^2 v_j^n, \tag{20}$$

where

$$v_j^n = \frac{1}{j}\sum_{i=0}^{j-1} |\Psi_i^n|^2 i^2 + \sum_{i=j}^{N-1} |\Psi_i^n|^2 i. \tag{21}$$

Since we now have all the parts of the Hamiltonian discretized, we can write the matrix Q in the following way:

$$Q = \begin{pmatrix} b_0 & c_0 & 0 & 0 & \cdots \\ a_1 & b_1 & c_1 & 0 & \cdots \\ 0 & a_2 & b_2 & c_2 & \\ \vdots & & & \vdots & \cdots \\ 0 & \cdots & & a_{N-1} & b_{N-1} \end{pmatrix}, \tag{22}$$

with

$$a_j = \beta\,\frac{j-1}{j} \quad \text{for} \quad 0 < j \leq N-1, \tag{23}$$

$$b_0 = \frac{1}{2} - 6\beta - \gamma v_0, \qquad b_j = \frac{1}{2} - 2\beta - \gamma v_j \quad \text{for} \quad 0 < j \leq N-1, \tag{24}$$

$$c_0 = 6\beta \qquad c_j = \beta\,\frac{j+1}{j} \quad \text{for} \quad 0 < j < N-1, \tag{25}$$

and γ and β being defined as

$$\beta = -\frac{i}{8m}\frac{\Delta t}{(\Delta r)^2} \qquad \text{and} \qquad \gamma = i\pi m^2(\Delta t)(\Delta r)^2. \tag{26}$$

Since matrix Q (22) is tridiagonal, the numerically efficient Thomas algorithm may be used do solve the system of equations (15). Then, the system evolution is obtained iterating expression (14).

Appendix 2: Comparison between our results and the literature

For the initial condition with only one Gaussian, Eq. (7), there are at least other two works that evaluated numerically the critical mass m_c. These two works, references [26,54], found a discrepancy of 20 % in its value. In this appendix we compare our results with the results of the reference [54] and show that our estimate for m_c agrees with this. We also discuss the possible sources of the discrepancy with the work [26].

In reference [54], Meter studies numerically four different values of mass. In Fig. 4 of [54] he shows the temporal evolution of r_p, from which we extract the average value $\langle r_p \rangle$. Figure 6 compares Meter's result with the value of $\langle r_p \rangle$ found for $R = 0$ in this work and shows a good agreement.

We cannot do the same comparison with the reference [26] because the authors did not compute the long time behaviour of the wave packet. In our Figs. 2 and 3, we observe that a long time series is necesssary to obtain the stationary solution. We

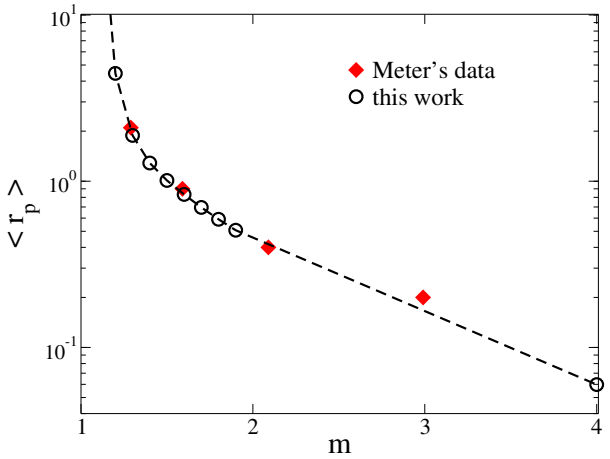

Fig. 6 Average value of r_p versus m for the initial condition with a single Gaussian. $\langle r_p \rangle$ is defined during the interval $\Delta t \in [2000t_r, 4000t_r]$. $\langle r_p \rangle$ is measured in units of σ, m in units of m_r, and the system size used in this simulation is $L = 10^4\sigma$. The *diamond symbols* are extracted from Fig. 4 of reference [54]

believe that this is the source of the discrepancy between both results. Another possible source of difference are finite size effects. The authors in reference [26] do not specify their system size, but it is possible that they used a relatively small system. As already noted in the main text, for the kind of boundary conditions we are employing – which is the same as the authors of the reference [26] – it is important to keep the system size big enough in order to avoid reflections of the wave packet at the system boundary.

Appendix 3: The critical mass

The expression for the critical mass obtained via the method of section 2 is

$$m_c = \left(\frac{A}{4B}\right)^{\frac{1}{3}},$$

where

$$\begin{aligned} A = \hbar^2 r_p^3(0)\Big(&8e^{\frac{r_p^2(0)+R^2}{\sigma^2}} R\sigma^4(2r_p^4(0) - 7r_p^2(0)\sigma^2 + 3\sigma^4) \\ &+ 4e^{\frac{r_p^2(0)+2R^2}{\sigma^2}} \sqrt{\pi}\sigma^3(2R^2+\sigma^2)(2r_p^4(0) - 7r_p^2(0)\sigma^2 + 3\sigma^4) \\ &+ 4e^{\frac{(r_p(0)+R)^2}{\sigma^2}} \sqrt{\pi}\sigma^5\big(2r_p^4(0) - 6r_p^3(0)R - 2R^2\sigma^2 + 3\sigma^4 \\ &+ r_p^2(0)(6R^2 - 7\sigma^2) + r_p(0)(-2R^3 + 9R\sigma^2)\big) \\ &+ 4e^{\frac{r_p^2(0)+2R^2}{\sigma^2}} \sqrt{\pi}\sigma^3(2R^2+\sigma^2)(2r_p^4(0) - 7r_p^2(0)\sigma^2 + 3\sigma^4)\,\mathrm{Erf}(R/\sigma) \end{aligned}$$

$$
\begin{aligned}
&+ e^{\frac{2r_p^2(0)+2r_p(0)R+3R^3}{2\sigma^2}} \pi^{\frac{1}{4}} \sqrt{s^3}\big(-8r_p^4(0)(R^2-2\sigma^2)+12r_p^3(0)(R^3-2R\sigma^2)\\
&+ r_p^2(0)(-6R^4+32R^2\sigma^2-56\sigma^4)+2\sigma^2(R^4-4R^2\sigma^2+12\sigma^4)\\
&+ r_p(0)(R^5-16R^3\sigma^2+36R\sigma^4)\big)\\
&\times\sqrt{\sigma\left(2e^{-\frac{R^2}{\sigma^2}}R\sigma+\sqrt{\pi}(2R^2+\sigma^2)+\sqrt{\pi}(2R^2+\sigma^2)\,\mathrm{Erf}(R/\sigma)\right)}\,\Big),
\end{aligned}
$$

and

$$
\begin{aligned}
B = G\sigma^6\Big(&2e^{\frac{r_p^2(0)+R^2}{\sigma^2}}R\sigma^2(2r_p^4(0)-5r_p^2(0)\sigma^2+\sigma^4)\\
&+ e^{\frac{r_p^2(0)+2R^2}{\sigma^2}}\sqrt{\pi}\sigma(2R^2+\sigma^2)(2r_p^4(0)-5r_p^2(0)\sigma^2+\sigma^4)\\
&+ e^{\frac{(r_p(0)+R)^2}{\sigma^2}}\sqrt{\pi}\sigma^3\big(2r_p^4(0)-4r_p^3(0)R+4r_p(0)R\sigma^2+\sigma^4+r_p^2(0)(2R^2-5\sigma^2)\big)\\
&+ e^{\frac{r_p^2(0)+2R^2}{\sigma^2}}\sqrt{\pi}\sigma(2R^2+\sigma^2)(2r_p^4(0)-5r_p^2(0)\sigma^2+\sigma^4)\,\mathrm{Erf}(R/\sigma)\\
&+ e^{\frac{2r_p^2(0)+2r_p(0)R+3R^2}{\sigma^2}}\pi^{\frac{1}{4}}\sqrt{\sigma^3}\big(4r_p^4(0)-4r_p^3(0)R+4r_p(0)R\sigma^2\\
&+ 2\sigma^4+r_p^2(0)(R^2-10\sigma^2)\big)\\
&\times\sqrt{\sigma\left(2e^{-\frac{R^2}{\sigma^2}}R\sigma+\sqrt{\pi}(2R^2+\sigma^2)+\sqrt{\pi}(2R^2+\sigma^2)\,\mathrm{Erf}(R/\sigma)\right)}\,\Big).
\end{aligned}
$$

Appendix 4: The limit $R \gg 1\sigma$

In order to investigate the behavior of the system when R is large, we first consider the situation where the initial condition is a single radially symmetric wave package at R, $\Psi(0,x)=\Psi_R(0,x)$. In this situation, it is easy to analytically estimate m_c exactly as in section 3.1 of [26]. Thus, we consider the free particle solution Eq. (2); find the value $r_p(t)$ of r for which the radial probability density $\varrho(t,r)=4\pi r^2|\Psi(t,x)|^2$ has a global maximum; compute the peak's acceleration at time zero, $\ddot{r}_p(0)$; and set it equal to $Gm/(r_p(0))^2$. This produces the following expression for the critical mass:

$$
m_c = \frac{(R^2\hbar^2+2\hbar^2\sigma^2+\hbar^2R\sqrt{R^2+4\sigma^2})^{\frac{1}{3}}}{(G\sigma^2)^{\frac{1}{3}}(R^2+4\sigma^2)^{\frac{1}{6}}}, \tag{27}
$$

which of course reduces to $m_r=\left(\frac{\hbar^2}{G\sigma}\right)^{\frac{1}{3}}$ when $R=0$. From the above expression it is clear that m_c increases with R. In particular, one *cannot decrease the critical mass using only a single Gaussian as the initial condition.*

We now show that the system "decouples" into two weakly interacting subsystems when R is large.

Suppose that Ψ is a solution to Eq. (1) with initial condition $\Psi(0,x) = \Psi_1(0,x) + \Psi_2(0,x)$. For simplicity, assume that $\Psi_1(0,x)$ and $\Psi_2(0,x)$ have compact and disjoint supports, i.e.,

$$\mathrm{supp}(\Psi_i(0)) \equiv \{x \in \mathbb{R}^3 \,|\, \Psi_i(0,x) \neq 0\} \subset B_{r_i}(0),$$

$i = 1, 2$, where $B_{r_i}(0)$ is the ball of radius $r_i > 0$ centered at the origin (strictly speaking, the support is the closure of the above set, but this will make no difference in our argument), and

$$\mathrm{supp}(\Psi_1(0)) \cap \mathrm{supp}(\Psi_2(0)) = \varnothing, \;\; |\,\mathrm{supp}(\Psi_1(0)) - \mathrm{supp}(\Psi_1(0))| \gg 1.$$

In our case the supports are not disjoint, but since we are interested in the case $R \gg 1$, this will be approximately the case. As Ψ is generally a well-behaved function of t, we can also assume that for small t, $\Psi \approx \Psi_1 + \Psi_2$, where $\Psi_i(t,x)$ is close to $\Psi_i(0,x)$ if t is very small. Thus we can also assume that

$$\mathrm{supp}(\Psi_1(t)) \cap \mathrm{supp}(\Psi_2(t)) = \varnothing, \;\; |\,\mathrm{supp}(\Psi_1(t)) - \mathrm{supp}(\Psi_1(t))| \gg 1 \tag{28}$$

(again, this will hold only as an approximation, but it suffices for our purposes). We restrict our attention to small t, because if confinement is going to happen due to the gravitational interaction, this should happen at earlier times before the wave-function has spread out considerably.

For $\Psi = \Psi_1 + \Psi_2$, Eq. (1) reads

$$\begin{aligned} i\hbar\frac{\partial\Psi_1}{\partial t} + i\hbar\frac{\partial\Psi_2}{\partial t} = &\left(-\frac{\hbar^2}{2m}\Delta - Gm^2\int_{\mathbb{R}^3}\frac{|\Psi_1|^2}{|x-y|}\,dy\right)\Psi_1 \\ &+\left(-\frac{\hbar^2}{2m}\Delta - Gm^2\int_{\mathbb{R}^3}\frac{|\Psi_2|^2}{|x-y|}\,dy\right)\Psi_2 \\ &-Gm^2\left(\int_{\mathbb{R}^3}\frac{|\Psi_1|^2}{|x-y|}\,dy\right)\Psi_2 - Gm^2\left(\int_{\mathbb{R}^3}\frac{|\Psi_2|^2}{|x-y|}\,dy\right)\Psi_1 \\ &-Gm^2\left(\int_{\mathbb{R}^3}\frac{\Psi_1\Psi_2^* + \Psi_1^*\Psi_2}{|x-y|}\,dy\right)(\Psi_1+\Psi_2). \end{aligned}$$

The cross terms $\Psi_1\Psi_2^*$ and $\Psi_1^*\Psi_2$ vanish, because for any given y, either $\Psi_1(t,y)$ or $\Psi_2(t,y)$ vanishes in light of expression (28).

If $x \in \mathrm{supp}(\Psi_1(t))$, then the term

$$-Gm^2\left(\int_{\mathbb{R}^3}\frac{|\Psi_1|^2}{|x-y|}\,dy\right)\Psi_2$$

vanishes, and the term

$$-Gm^2\left(\int_{\mathbb{R}^3}\frac{|\Psi_2|^2}{|x-y|}\,dy\right)\Psi_1$$

will be very small since

$$\int_{\mathbb{R}^3} \frac{|\Psi_2|^2}{|x-y|}\,dy = \int_{\mathrm{supp}(\Psi_2(t))} \frac{|\Psi_2|^2}{|x-y|}\,dy,$$

and x and $\mathrm{supp}(\Psi_2(t))$ are very far away, so that $|x-y|$ is very large.

A similar statement holds if $x \in \mathrm{supp}(\Psi_2(t))$ instead, and obviously all terms vanish if $x \notin \mathrm{supp}(\Psi_1(t)) \cup \mathrm{supp}(\Psi_2(t))$. Thus

$$\begin{aligned} i\hbar\frac{\partial\Psi_1}{\partial t} + i\hbar\frac{\partial\Psi_2}{\partial t} \approx &\left(-\frac{\hbar^2}{2m}\Delta - Gm^2\int_{\mathbb{R}^3}\frac{|\Psi_1|^2}{|x-y|}\,dy\right)\Psi_1 \\ &+\left(-\frac{\hbar^2}{2m}\Delta - Gm^2\int_{\mathbb{R}^3}\frac{|\Psi_2|^2}{|x-y|}\,dy\right)\Psi_2, \end{aligned}$$

i.e., under the above circumstances, the evolution behaves as if the system were linear. Thus if one considers the situation where $\Psi_1(0,x) \approx \Psi_0(0,x)$ and $\Psi_2(0,x) \approx \Psi_R(0,x)$, with $R \gg 1$, a very large value of m is necessary to confine the part of the wave function associated with Ψ_2 [recall Eq. (27)]. Hence, confinement happens essentially due to Ψ_1, which in this case corresponds roughly to the system with a single Gaussian centered at the origin. This explains why m_c approaches m_r when R is very large.

Acknowledgments Marcelo M. Disconzi is partially supported by NSF award 1305705. Marion Silvestrini, leonardo G. Brunnet and Carolina Brito thank the Brazilian funding agencies CNPq, Capes and Fapergs. We thank the supercomputing laboratory at IF-UFRGS and at New York University, where the simulations were run, for computer time.

References

1. Anastopoulos, C., Hu, B.L.: Problems with the Newton–Schrödinger equations? New J. Phys. **16**, 085007 (2014)
2. Andriot, D., Goi, E., Minasian, R., Petrini, M.: Supersymmetry breaking branes on solvmanifolds and de sitter vacua in string theory. J. High Energy Phys. **2011**(5), 1–65 (2011)
3. Arndt, M., Hornberger, K., Zeilinger, A.: Probing the Limits of the Quantum World. Phys. World. **18**, 35–40 (2005)
4. Baumann, D., McAllister, L.: Inflation and String Theory. arXiv preprint arXiv: arXiv:1404.2601
5. Becker, K., Becker, M., Schwarz, J.H.: String Theory and M-Theory: A Modern Introduction. Cambridge University Press, Cambridge (2007)
6. Benguria, R., Brézis, H., Lieb, E.H.: The Thomas–Fermi–von Weizsäcker theory of atoms and molecules. Commun. Math. Phys. **79**(2), 167–180 (1981)
7. Blau, M., Theisen, S.: String theory as a theory of quantum gravity: a status report. Gen. Relativ. Gravit. **41**(4), 743–755 (2009)
8. Burrage, C., Copeland, E.J., Hinds, E.A.: Probing Dark Energy with Atom Interferometry. arXiv preprint arXiv:1408.1409 (2014)
9. Candelas, P., Horowitz, G.T., Strominger, A., Witten, E.: Vacuum configurations fr superstrings. Nucl. Phys. B **258**, 46–74 (1985)
10. Carlip, S.: Quantum Gravity in 2+1 Dimensions. Cambridge University Press, Cambridge (1998)
11. Carlip, S.: Is quantum gravity necessary? Class. Quant. Gravit. **25**, 154010 (2008)
12. Cazenave, T., Lions, P.-L.: Orbital stability of standing waves for some nonlinear Södinger equations. Commun. Math. Phys. **85**(4), 549–561 (1982)

13. Chiou, D.-W.: Loop quantum gravity. Int. J. Mod. Phys. D **24**(1), 1530005 (2015)
14. Cingolani, S., Clapp, M., Secchi, S.: Multiple solutions to a magnetic nonlinear Choquard equation. Z. Angew. Math. Phys. **63**(2), 233–248 (2012)
15. Clapp, M., Salazar, D.: Positive and sign changing solutions to a nonlinear Choquard equation. J. Math. Anal. Appl. **407**(1), 1–15 (2013)
16. Dabholkar, S.P., Disconzi, M.M., Pingali, V.P.: Remarks on positive energy vacua via effective potentials in string theory. Lett. Math. Phys. **104**(7), 893–910 (2014)
17. Disconzi, M.M.: A note on quantization in the presence of gravitational shock waves. Mod. Phys. Lett. A **28**(31), 1350111 (2013)
18. Disconzi, M.M.: Some a priori estimates for a critical Schrodinger–Newton equation. In: Electronic Journal of Differential Equations, Ninth MSU-UAB Conference, vol. 20, pp. 39–51 (2013)
19. Disconzi, M.M., Douglas, M.R., Pingali, V.: On the boundedness of effective potentials arising from string compactifications. Commun. Math. Phys. **325**(3), 847–878 (2014)
20. Douglas, M.R.: Effective potential and warp factor dynamics. J. High Energy Phys. **2010**(3), 1–32 (2010)
21. Douglas, M.R., Kachru, S.: Flux compactification. Rev. Mod. Phys. **79**, 733–796 (2007)
22. Douglas, M.R., Kallosh, R.: Compactification on negatively curved manifolds. J. High Energy Phys. **2010**(6), 1–18 (2010)
23. Fulling, S.A.: Aspects of Quantum Field Theory in Curved Spacetime, vol. 17. Cambridge University Press, Cambridge (1989)
24. Gidas, B., Ni, W.M., Nirenberg, L.: Symmetry of positive solutions of nonlinear elliptic equations in rn. Adv. Math. Suppl. Stud. A **7**, 369–402 (1981)
25. Ginibre, J., Velo, G.: On a class of non linear Schrödinger equations with non local interaction. Math. Z. **170**(2), 109–136 (1980)
26. Giulini, D., Großardt, A.: Gravitationally induced inhibitions of dispersion according to the Schrödinger–Newton equation. Class. Quantum Gravit. **28**(19), 195026 (2011)
27. Giulini, D., Großardt, A.: Class. Quantum Gravit. **29**, 215010 (2012)
28. Giulini, D., Großardt, A.: Centre-of-mass motion in multi-particle Schrödinger–Newton dynamics. New J. Phys. **16**(7), 075005 (2014)
29. Grana, M.: Flux compactifications in string theory: a comprehensive review. Phys. Rep. **423**(3), 91–158 (2006)
30. Green, M.B., Schwarz, J.H., Witten, E.: Superstring Theory, vol. 1, 2. Cambridge University Press (1987)
31. Hackermüller, L., Uttenthaler, S., Hornberger, K., Reiger, E., Brezger, B., Zeilinger, A., Arndt, M.: Wave nature of biomolecules and fluorofullerenes. Phys. Rev. Lett. **91**(9), 090408 (2003)
32. Hawking, S.W.: Particle creation by black holes. Commun. Math. Phys. **43**(3), 199–220 (1975)
33. Kachru, S., Kallosh, R., Linde, A., Trivedi, S.P.: De sitter vacua in string theory. Phys. Rev. D **68**, 046005 (2006)
34. Lions, P.L.: The Choquard equation and related questions. Nonlinear Anal.: Theory Methods Appl. **4**(6), 1063–1072 (1980)
35. Lions, P.L.: Compactness and topological methods for some nonlinear variational problems of mathematical physics. N.-Holl. Math. Stud. **61**, 17–34 (1982)
36. Ma, L., Zhao, L.: Classification of positive solitary solutions of the nonlinear Choquard equation. Arch. Ration. Mech. Anal. **195**(2), 455–467 (2010)
37. Manfredi, G.: The Schrödinger–Newton equations beyond Newton. Gen. Relativ. Gravit. **47**(2), 1–12 (2015)
38. Moroz, V., Van Schaftingen, J.: Groundstates of nonlinear Choquard equations: existence, qualitative properties and decay asymptotics. J. Funct. Anal. **265**(2), 153–184 (2013)
39. Parker, L., Toms, D.: Quantum Field Theory in Curved Spacetime: Quantized Fields and Gravity. Cambridge University Press, Cambridge (2009)
40. Penrose, R.: Twistor algebra. J. Math. Phys. **8**(2), 345–366 (1967)
41. Penrose, R.: On the origins of twistor theory. Gravit. Geom. 341–361 (1987)
42. Penrose, R.: On gravity's role in quantum state reduction. Gen. Relativ. Gravit. **28**(5), 581–600 (1996)
43. Penrose, R.: Quantum computation, entanglement and state reduction. In: Philosofical Transactions-Royal Society of Londo Series A Mathematical Physical and Engineering Sciences, pp. 1927–1937 (1998)
44. Penrose, R.: The central programme of twistor theory. Chaos Solitons Fract. **10**(2), 581–611 (1999)

45. Polchinski, J.: String theory, vols. 1 and 2, vol. 402, p. 531. Cambridge University Press, Cambridge (1998)
46. Press, W.H., Teukolsky, S.A., Vetterling, W.T., Flannery, B.P.: Numerical Recipes in C: The Art of Scientific Computing. Cambridge University Press, Cambridge (1992)
47. Rabinowitz, P.H.: On a class of nonlinear Schrödinger equations. Z. Angew. Math. Phys. **43**(2), 270–291 (1992)
48. Rovelli, C.: Quantum Gravity. Cambridge University Press, Cambridge (2004)
49. Rovelli, C.: Covariant Loop Quantum Gravity: An Elementary Introduction to Quantum Gravity and Spinfoam Theory. Cambridge University Press, Cambridge (2014)
50. Salzman, P.J., Carlip, S.: A Possible Experimental Test of Quantized Gravity. arXiv preprint gr-qc/0606120 (2006)
51. Shatah, J., Strauss, W.: Instability of nonlinear bound states. Commun. Math. Phys. **100**(2), 173–190 (1985)
52. Shomer, A.: A Pedagogical Explanation for the Non-renormalizability of Gravity. arXiv preprint arXiv:0709.3555 (2007)
53. Silverstein, E.: Simple de sitter solutions. Phys. Rev. D **77**(10), 106006 (2008)
54. van Meter, J.R.: Schrödinger–Newton "collapse of the wave function". Class. Quant. Gravit. **28**, 215013 (2011)
55. Wald, R.M.: Quantum Field Theory in Curved Spacetime and Black Hole Thermodynamics (Chicago Lectures in Physics). University of Chicago Press (1994)
56. Wald, R.M.: General Relativity. University of Chicago Press, Chicago (2010)